JCI The Journal of Clinical Investigation

Loss of Gata5 in mice leads to bicuspid aortic valve

Brigitte Laforest, … , Gregor Andelfinger, Mona Nemer

J Clin Invest. 2011;121(7):2876-2887. https://doi.org/10.1172/JCI44555.

Research Article Cardiology

Bicuspid aortic valve (BAV), the leading congenital heart disease, occurs in 1%–2% of the population. Genetic studies suggest that BAV is an autosomal-dominant disease with reduced penetrance. However, only 1 gene, *NOTCH1*, has been linked to cases of BAV. Here, we show that targeted deletion of *Gata5* in mice leads to hypoplastic hearts and partially penetrant BAV formation. Endocardial cell–specific inactivation of *Gata5* led to BAV, similar to that observed in $Gata5^{-/-}$ mice. In all cases, the observed BAVs resulted from fusion of the right-coronary and noncoronary leaflets, the subtype associated with the more severe valve dysfunction in humans. Neither endocardial cell proliferation nor cushion formation was altered in the absence of *Gata5*. Rather, defective endocardial cell differentiation, resulting from the deregulation of several components of the Notch pathway and other important endocardial cell regulators, may be the underlying mechanism of disease. The results unravel a critical cell-autonomous role for endocardial *Gata5* in aortic valve formation and identify *GATA5* as a potential gene responsible for congenital heart disease in humans. Mice with mutated *Gata5* alleles represent unique models to dissect the mechanisms underlying degenerative aortic valve disease and to develop much-needed preventive and therapeutic interventions.

Loss of Gata5 in mice leads to bicuspid aortic valve

Brigitte Laforest,[1] Gregor Andelfinger,[2] and Mona Nemer[1,3]

[1]Program in Molecular Biology and [2]Department of Pediatrics, University of Montreal, Montreal, Quebec, Canada.
[3]Department of Biochemistry, Microbiology and Immunology, University of Ottawa, Ottawa, Ontario, Canada.

Bicuspid aortic valve (BAV), the leading congenital heart disease, occurs in 1%–2% of the population. Genetic studies suggest that BAV is an autosomal-dominant disease with reduced penetrance. However, only 1 gene, *NOTCH1*, has been linked to cases of BAV. Here, we show that targeted deletion of *Gata5* in mice leads to hypoplastic hearts and partially penetrant BAV formation. Endocardial cell–specific inactivation of *Gata5* led to BAV, similar to that observed in *Gata5*$^{-/-}$ mice. In all cases, the observed BAVs resulted from fusion of the right-coronary and noncoronary leaflets, the subtype associated with the more severe valve dysfunction in humans. Neither endocardial cell proliferation nor cushion formation was altered in the absence of *Gata5*. Rather, defective endocardial cell differentiation, resulting from the deregulation of several components of the Notch pathway and other important endocardial cell regulators, may be the underlying mechanism of disease. The results unravel a critical cell-autonomous role for endocardial *Gata5* in aortic valve formation and identify *GATA5* as a potential gene responsible for congenital heart disease in humans. Mice with mutated *Gata5* alleles represent unique models to dissect the mechanisms underlying degenerative aortic valve disease and to develop much-needed preventive and therapeutic interventions.

Introduction

Proper formation and function of the heart valves is critical for unidirectional blood flow within the 4-chambered mammalian heart, and valve dysfunction leads to serious cardiovascular complications. Valve disease, whether congenital or acquired, is a major clinical problem worldwide, and valve replacement is the second leading cardiac surgery in North America.

Bicuspid aortic valve (BAV) is the most common congenital cardiac malformation, occurring in 1%–2% of the population (1). It is generally diagnosed in adulthood when deterioration of the abnormal leaflets becomes clinically evident, with affected individuals developing valve disease 10 years earlier than those with normal aortic valve (AV) leaflets. Patients with BAV are at increased risks of developing serious complications, including aortic stenosis, aortic regurgitation, and endocarditis; one-third of these patients will in fact develop significant cardiovascular complications, and many will require surgical interventions. Population studies have suggested that BAV may be responsible for more mortality and morbidity than all other congenital heart diseases (CHDs) combined (2). Despite this, our understanding of the mechanisms underlying BAV formation remains limited. BAVs occur either in isolation or in association with other malformations, such as coarctation of the aorta, ventricular septal defects, and hypoplastic LV (3–5). Genetic studies have established that BAV is a highly heritable trait with autosomal-dominant transmission and incomplete penetrance (6, 7). Thus far, only 1 gene, *NOTCH1*, has been linked to BAV in humans, with mutations found in some but not all BAVs (8, 9). Genome-wide scans have suggested linkages to several human chromosomal regions, but no other disease-causing genes have yet been identified (10). In animal models, BAVs have been found in a subset of mice lacking endocardial nitric oxide synthase (*Nos3*) or the cardiac transcription factor Nkx2.5, but neither gene has been associated yet with human BAV (11, 12). Better knowledge of the molecular pathways governing valve development may help identify BAV-causing genes.

Over the past years, molecular and genetic analysis of heart development have started to identify genes and pathways involved at various stages of valvulogenesis (13). Valve development is a complex process that involves expansion and differentiation of endocardial cells (ECs) and their migration after epithelial-to-mesenchymal transformation (EMT) to form endocardial cushions at the atrioventricular canal (AVC) and within the outflow tract (OFT). The atrioventricular cushions then give rise to the mitral and tricuspid valves, whereas the AV and pulmonary valve arise from the OFT. In addition to ECs, other cell types participate in valve development, notably neural crest and secondary heart field–derived cells, which play important roles in the formation of the OFT. Bone morphogenetic proteins Bmp2 and Bmp4 are critical myocardially derived signals that modulate the EMT. BMP and BMP-regulated transcription factors can promote both proliferation and differentiation of ECs and are part of a complex regulatory network that must tightly regulate cell-cell interactions and cell fate throughout valvulogenesis. Mice lacking components of the BMP pathway or transcription factors that control the proliferation and differentiation of ECs, such as Twist1, Msx, or the Notch target Slug1, have defective EMT. Similarly, proper levels of VEGF are needed to promote proliferation and survival of ECs prior to EMT (14, 15).

Another critical pathway for valve development is Notch, which plays multiple roles throughout valvulogenesis. Notch1, Notch2, Notch4, and the Notch ligands Dll4 and Jag1 are expressed in ECs, where they regulate endocardial differentiation and EMT. The importance of this pathway is underscored by the finding that mutations of *NOTCH1* are linked with human BAV and that mutations in *JAG1* and *NOTCH2* cause Alagille syndrome, an autosomal-dominant disease that affects the cardiac OFT (16–18). *JAG1* mutations have also been identified in other forms of CHD with EC involvement (19, 20).

Conflict of interest: The authors have declared that no conflict of interest exists.
Citation for this article: *J Clin Invest.* 2011;121(7):2876–2887. doi:10.1172/JCI44555.

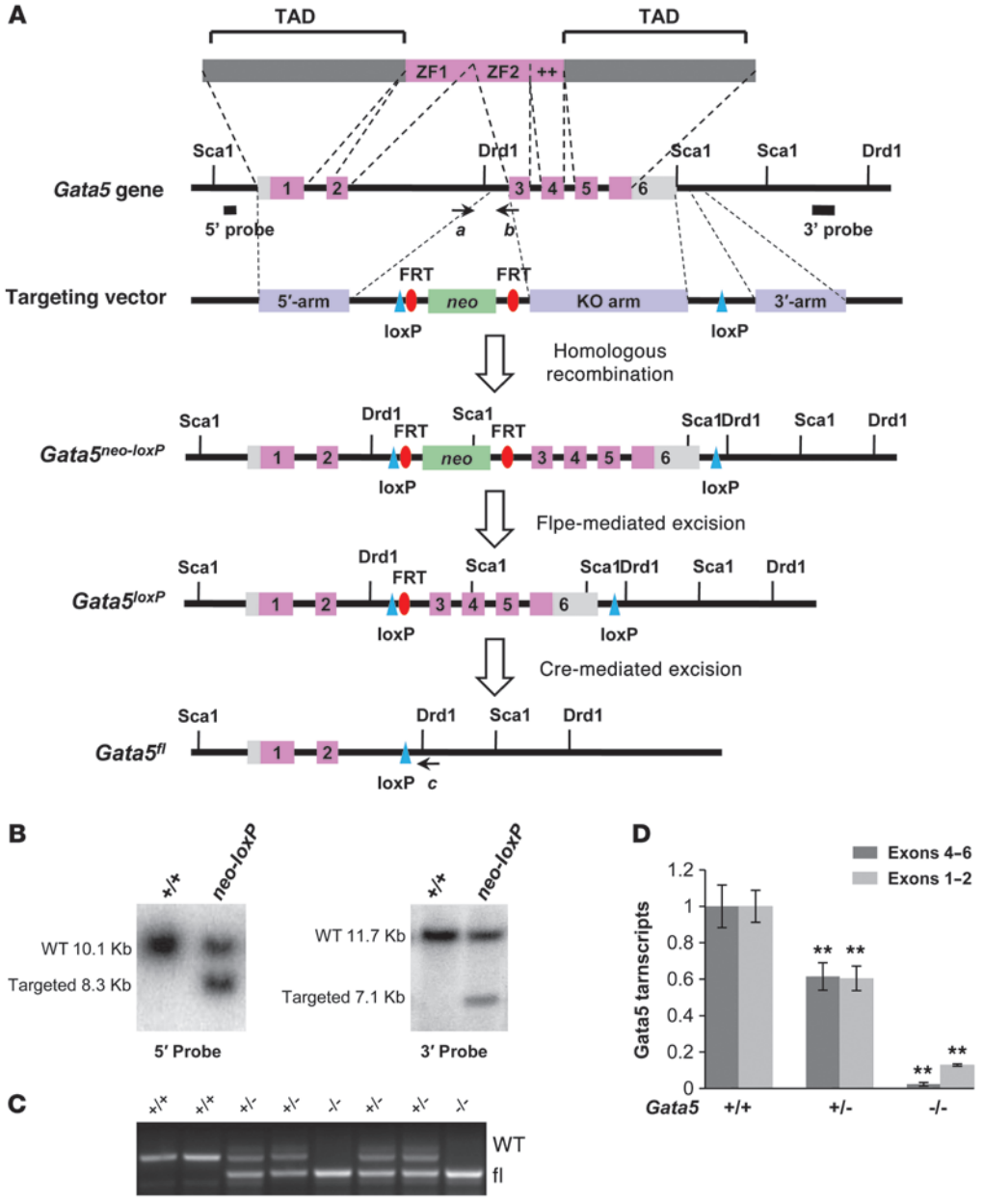

Figure 1

Generation of a *Gata5*-null allele. (**A**) *Gata5* locus and targeting strategy. Positions of the 5′ and 3′ probes used for Southern blots are shown. Cre-mediated excision removes exons 3–6, leaving 1 loxP site. Coding exons are in pink; noncoding exons are in gray. FRT, Flp recombination target; TAD, transactivation domain; ZF, zinc finger. (**B**) Southern blot analysis of targeted ES cells. Genomic DNA was digested with Sca1 and hybridized to the 5′ probe, or digested with Drd1 and hybridized to a 3′ probe. (**C**) Genotyping of WT (+/+), heterozygous (+/–), and homozygous (–/–) targeted allele. PCR using primers a–b and a–c (as in **A**) identified product corresponding to WT (448 bp) and floxed (285 bp) alleles. (**D**) Q-PCR of *Gata5* transcripts in hearts of embryos at E12.5. Results demonstrate complete reduction of Gata5 exon 4–6 and exon 1–2 in *Gata5*$^{-/-}$ mice. *Gapdh* was used as an internal control. $^{**}P < 0.01$ vs. *Gata5*$^{+/+}$.

Notch proteins are cell surface receptors that are cleaved by γ-secretase complex upon ligand binding, releasing the Notch1 intracellular domain (NICD), which then translocates to the nucleus, associating with recombination signal binding protein for immunoglobulin κ J region (Rbpjκ) to switch it from a transcriptional repressor to an activator. Notch target genes include transcription factors as well as signaling molecules such as neuregulin, VE-cadherin, and the basic helix-loop-helix proteins Hey and Hrt, which regulate BMP signaling. Consistent with a critical role for the Notch pathway in endocardial cushion development, inactivation of several pathway components in mice produce cardiac defects (21). Endocardial Notch signaling is also required for endocardial-myocardial interactions, specifically in ventricular trabeculation, and may potentially explain the link between BAV and hypoplastic LVs (22).

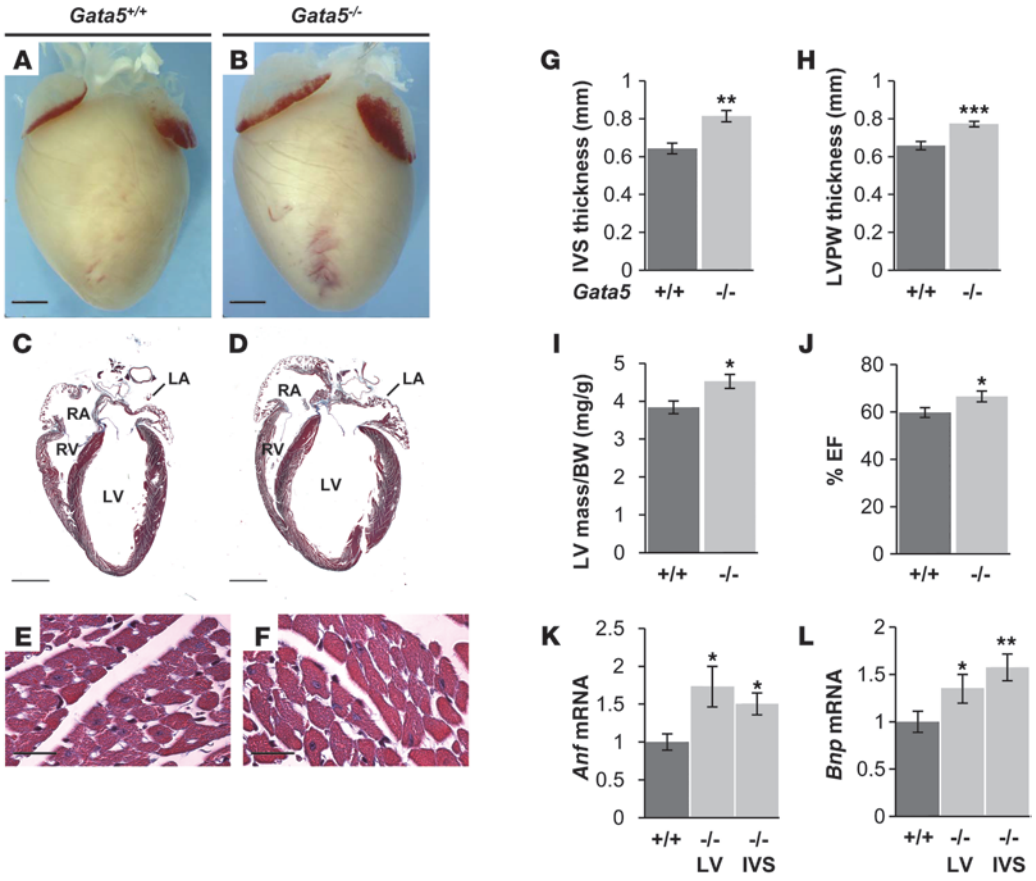

Figure 2
Mild LV hypertrophy of *Gata5*$^{-/-}$ mice. (**A**–**D**) Anatomical analysis of *Gata5*$^{+/+}$ and *Gata5*$^{-/-}$ mice. (**A** and **B**) Frontal view orientation of the hearts showed a mild increase in *Gata5*$^{-/-}$ mouse heart size. (**C** and **D**) Trichrome staining demonstrated increased heart size, right atrial enlargement, and increased LV internal dimension of *Gata5*$^{-/-}$ mice. LA, left atrium; RA, right atrium. (**E** and **F**) High-magnification views of cardiomyocytes, showing increased cell size in *Gata5*$^{-/-}$ mice. (**G**–**I**) Echocardiography of *Gata5*$^{+/+}$ and *Gata5*$^{-/-}$ mice at 70 days of age (n = 11–13 per group) demonstrated increased thickness of the IVS (**G**) and LV posterior wall (LVPW; **H**) and increased LV mass (**I**) in *Gata5*$^{-/-}$ mice, suggesting the presence of LV hypertrophy. (**J**) Echocardiography at 70 days of age showed increased ejection fraction (EF) in *Gata5*$^{-/-}$ mice (n = 11–13 per group). (**K** and **L**) Enhanced *Anf* and *Bnp* expression in *Gata5*$^{-/-}$ LV and IVS, as revealed by Q-PCR at 30 days of age (n = 6–8 per group). Scale bars: 1,500 μm (**A**–**D**); 20 μm (**E** and **F**). $^{*}P < 0.05$, $^{**}P < 0.01$, $^{***}P < 0.001$.

Other families of transcription factors are present in ECs and regulate endocardial differentiation and valve formation. They include the forkhead proteins FoxP1 and Foxc2 as well as the SOX proteins Sox4 and Sox9 (23–25). Tbox proteins have also emerged as important regulators of valvulogenesis; Tbx2 and Tbx3 are required for establishing the AV boundary, whereas Tbx20 promotes EC expansion and differentiation (26–28). Finally, genetic and biochemical studies have suggested important roles for members of the GATA family of zinc finger proteins in EC expansion and differentiation. Tissue-specific deletion of *Gata4* in endothelial cells causes embryonic lethality by E12.5 because of defects in EMT, resulting in the formation of hypocellular endocardial cushion (29). In humans, mutations in *GATA4* have been found in association with septal defects (30–32). More recently, mutations in another GATA gene, *GATA6*, which in the heart is expressed predominantly in myocytes as well as neural crest–derived cells, have been reported in human CHD (33). In contrast to Gata4, which is expressed in both myocardial cells and ECs, Gata5 expression in the heart is largely restricted to ECs, where it is transiently expressed during embryonic development (34, 35). In vitro studies revealed a requirement for Gata5 for differentiation of committed cardiogenic precursors into endothelial ECs (36). In zebrafish, *faust* (which encodes Gata5) mutants lack ECs and have a reduced number of myocytes (37).

In this study, we show that targeted inactivation of *Gata5* in mice affected heart development and led to BAV. Deletion of Gata5 specifically from ECs was sufficient to recapitulate the cardiac phenotype of *Gata5*$^{-/-}$ mice, suggestive of a cell-autonomous function of Gata5 in regulating endocardial cushion differentiation. Mechanistically, we found that Gata5 regulated several pathways associated with EC differentiation, including Bmp4, Tbx20, Nos3, and Notch. Together, the data reveal an important function for Gata5 in AV development and identify *Gata5* as an important regulator of mammalian heart development and a candidate CHD causing gene.

Results

Gata5$^{-/-}$ *mice have mild LV hypertrophy*. The mouse *Gata5* gene contains 6 exons and spans 10 kbp of DNA. We generated the targeted allele by introducing loxP sites flanking exon 3 and exon 6

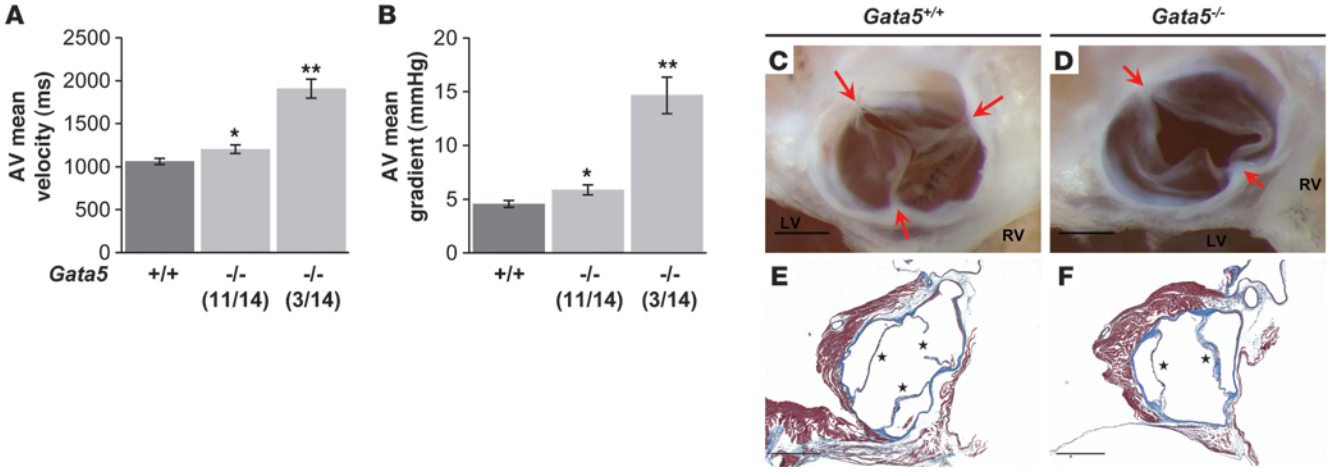

Figure 3
Valvular dysfunction of *Gata5*$^{-/-}$ mice. (**A** and **B**) Echocardiography of *Gata5*$^{+/+}$ and *Gata5*$^{-/-}$ mice at 70 days of age showed increased mean velocity and pressure gradients through the AV (n = 11–14 per group; the *Gata5*$^{-/-}$ group is shown divided because the 3 *Gata5*$^{-/-}$ mice with higher AV mean gradient were the mice with BAVs). (**C** and **D**) Anatomical analysis of *Gata5*$^{-/-}$ mice revealed the presence of BAV and tricuspid AV. Arrows indicate the point of attachment of the valve cups to the aortic wall. (**E** and **F**) Trichrome staining of the AV of *Gata5*$^{-/-}$ mice, showing the presence of 2 or 3 leaflets (asterisks). Scale bars: 500 μm. *P < 0.05, **P < 0.01.

through homologous recombination in ES cells (Figure 1A). These exons encode the second zinc finger essential for DNA binding, the nuclear localization sequence, and the complete C terminus. The presence of the targeted allele in ES cells was confirmed by Southern blot (Figure 1B). PCR analysis confirmed the presence of the WT (448 bp) or floxed (285 bp) alleles (Figure 1C). Mice heterozygous for *Gata5*$^{neo\text{-}loxP}$ were bred to CMV-cre females, which deletes in the germline, resulting in *Gata5*$^{+/-}$ mice. *Gata5*$^{+/-}$ mice were intercrossed to generate *Gata5*$^{-/-}$ mice on a 129/C57BL/6 mixed genetic background. *Gata5*$^{+/-}$ mice were viable and obtained at the expected Mendelian ratios. Quantitative PCR (Q-PCR) analysis at E12.5 confirmed that exons 3–6 had been deleted in *Gata5*$^{-/-}$ mice (Figure 1D). The presence of the first coding exon in the *Gata5* targeted allele ensured that a truncated protein containing the N-terminal portion of Gata5 could still be produced. However, Q-PCR analysis indicated a 90% reduction in transcripts from the first 2 coding exons in *Gata5*$^{-/-}$ mice (Figure 1D), which suggests that no Gata5 protein is likely to be produced as a consequence of nonsense-mediated mRNA decay.

Anatomical examination of *Gata5*$^{-/-}$ mice revealed a cardiac phenotype: at first sight, right atrial enlargement was visible, and heart size appeared mildly increased (Figure 2, A–D). Echocardiography as well as measurement of heart weight and ventricular mass confirmed that *Gata5*$^{-/-}$ hearts were larger than those of control littermates. Echocardiography performed on sex-matched *Gata5*$^{+/+}$ and *Gata5*$^{-/-}$ mice at 70 days (n = 11–14 per group) revealed increased interventricular septum (IVS) thickness (0.643 ± 0.028 mm vs. 0.814 ± 0.030 mm, P = 0.002), LV posterior wall thickness (0.658 ± 0.021 mm vs. 0.772 ± 0.014 mm, P < 0.001), and LV mass (3.840 ± 0.168 mg/g vs. 4.524 ± 0.183 mg/g, P < 0.05) in *Gata5*$^{-/-}$ hearts (Figure 2, G–I). Identical results were also obtained at 180 days (data not shown). The ejection fraction, a measure of LV performance, was slightly but consistently higher in *Gata5*$^{-/-}$ hearts (57.752% ± 2.061% vs. 66.570% ± 2.271%, P = 0.019; Figure 2J), suggestive of a hypercontractile state. Histological analysis and myocyte counts indicated that the increased mass was caused by myocyte enlargement, not hyperplasia (Figure 2, E and F). In fact, *Gata5*$^{-/-}$ ventricles had fewer myocytes per field than did control littermates (19 ± 2.5 cells vs. 28 ± 0.88 cells; P = 0.03). Increased *Anf*, *Bnp*, and *Acta* mRNA levels were observed as early as 30 days in the LV and IVS of *Gata5*$^{-/-}$ mice (Figure 2, K and L, and data not shown), consistent with the presence of LV hypertrophy.

Dysregulated cardiac morphogenesis and BAV in Gata5$^{-/-}$ *mice*. Since Gata5 is highly expressed in endocardial cushions of both OFT and AVC, we next determined whether its deletion disrupts valve formation or function. Hemodynamic evaluation of *Gata5*$^{-/-}$ mice at 70 days showed increased velocity and pressure gradients at the level of the mitral valve, AV, and pulmonary valve (Figure 3, A and B, and data not shown), suggestive of valve disease, which could contribute to development of ventricular hypertrophy. Analysis of the aortic root area revealed a significant decrease in *Gata5*$^{-/-}$ mice relative to *Gata5*$^{+/+}$ littermates (n = 11–14 per group) indicative of mild aortic stenosis; this was evident as early as 70 days (1.26 ± 0.05 mm^2 vs. 1.13 ± 0.05 mm^2, P < 0.05) and was further accentuated in 180-day-old mice (1.51 ± 0.05 mm^2 vs. 1.34 ± 0.04 mm^2, P < 0.05). Furthermore, 21% of *Gata5*$^{-/-}$ mice (3 of 14) had a much higher velocity (1,061.757 ± 35.480 mm/s vs. 1,906 ± 110.620 mm/s, P < 0.01) and gradient (4.569 ± 0.313 mmHg vs. 14.653 ± 1.704 mmHg, P = 0.015) through the AV (Figure 3, A and B). Morphologic examination of the valves revealed the presence of BAVs in 25% (7 of 28) of *Gata5*$^{-/-}$ mice compared with 3% (1 of 29) of *Gata5*$^{+/+}$ mice (Figure 3, C–F, and Table 1). No other structural abnormalities were evident at the level of the other valves or the septa. Thus, Gata5 seems to be essential for normal AV development.

Table 1
BAV incidence in *Gata5*$^{+/+}$ and *Gata5*$^{-/-}$ mice

Genotype	Total mice	Mice with BAV	Incidence
Gata5$^{+/+}$	29	1	3%
Gata5$^{-/-}$	28	7	25%

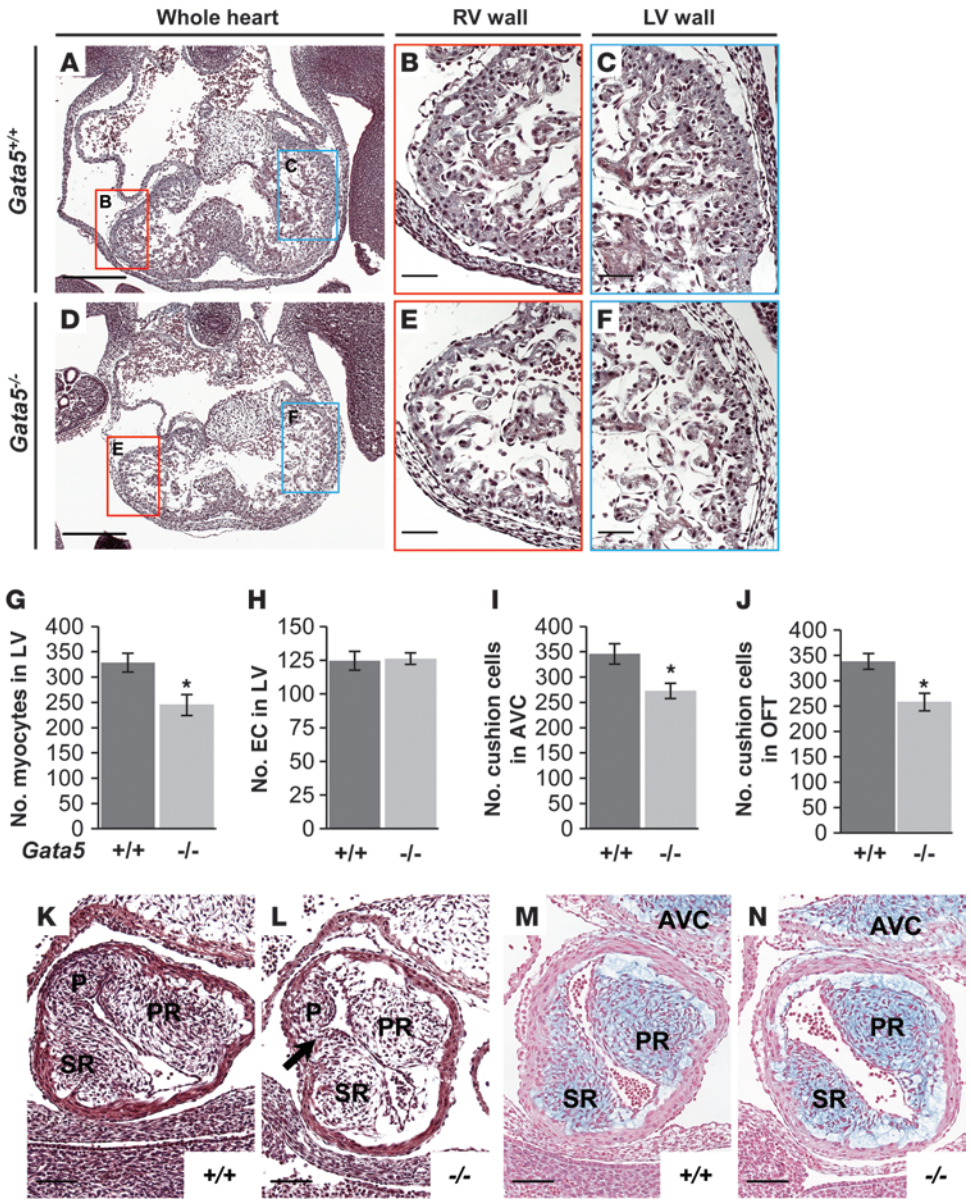

Figure 4
Reduced trabeculation and R-N BAV in *Gata5*$^{-/-}$ embryos. (**A**–**F**) Trichrome staining of heart transverse sections at E11.5. *Gata5*$^{-/-}$ embryos had thinner LV and RV and were less trabeculated than were *Gata5*$^{+/+}$ controls. Boxed regions in **A** and **D** are shown at higher magnification in **B**, **C**, **E**, and **F**, as indicated. (**G**–**J**) Number of cells in *Gata5*$^{-/-}$ and littermate *Gata5*$^{+/+}$ embryos at E11.5 (n = 3–5 per group). The number of myocytes within the LV was reduced in *Gata5*$^{-/-}$ mice compared with controls (**G**), whereas the number of ECs remained unchanged (**H**). The number of mesenchymal cells in the AVC and OFT of *Gata5*$^{-/-}$ embryos was also significantly decreased by 20% (**I** and **J**). (**K** and **L**) Trichrome staining of transverse sections of OFT at E11.5. Arrow denotes abnormal fusion of the posterior intercalated cushion with the septal ridge, creating a R-N BAV. SR, septal ridge; P, posterior intercalated cushion; PR, parietal ridge. (**M** and **N**) Alcian blue staining was used to visualize acid glycosaminoglycans, such as hyaluronic acid, within the endocardial cushions of the OFT. *Gata5*$^{-/-}$ embryos had a similar amount of alcian blue staining in the OFT endocardial cushions at E11.5. Scale bars: 300 μm (**A** and **D**); 50 μm (**B**, **C**, **E**, and **F**); 75 μm (**K**–**N**). *P < 0.05 vs. *Gata5*$^{+/+}$.

To determine whether the postnatal hypertrophy of *Gata5*$^{-/-}$ mice is present in embryonic hearts or whether it reflects a compensatory mechanism, the cardiac phenotype of *Gata5*$^{-/-}$ embryos was carefully analyzed. At E11.5, both LV and RV walls were thinner in *Gata5*$^{-/-}$ embryos than in control littermates (Figure 4, A–F). Moreover, *Gata5*$^{-/-}$ hearts were hypotrabeculated compared with their controls. To determine whether these changes were caused by a reduced number of myocytes and/or ECs, we counted both cell types using ImageJ software. A significant decrease in the number of myocytes (328.497 ± 18.565 cells vs. 244.667 ± 20.701 cells, P = 0.011), but not ECs, was evident in the LV of *Gata5*$^{-/-}$ versus *Gata5*$^{+/+}$ embryos (Figure 4, G and H). Thus, during development, lack of Gata5 results in hypoplastic hearts, which likely undergo compensatory hypertrophy postnatally.

The valve leaflets of the heart and IVS originate from the endocardial cushions, in which Gata5 expression is enriched. Cushion formation is localized to the OFT, where the pulmonary valve and AV will form, and in the AVC, which is responsible for mitral and tricuspid valve formation. We found that the number of mesenchymal cells was reduced in both the AVC (345.867 ± 20.066 cells vs. 272.667 ± 15.059 cells, P = 0.021; Figure 4I) and the OFT (338.333 ± 15.542 cells vs. 258.000 ± 17.387 cells, P = 0.032; Figure 4J), raising the possibility of reduced survival, proliferation, or migration of mesenchymal cells within the endocardial cushions. TUNEL assays and phosphohistone H3 immunostaining were carried out on E11.5 tissue sections to measure cell apoptosis and proliferation. No significant changes in either AVC or OFT were detected between *Gata5*$^{-/-}$ and control embryos. Therefore, we analyzed morphogenesis of the OFT cushions in more detail. The OFT cushions were formed properly in *Gata5*$^{-/-}$ embryos with reduced numbers of mesenchymal cells (Figure 4, K and L). The septal ridge was abnormally fused with the posterior intercalated cushion, leading to fusion of the right-coronary and noncoronary valve leaflets (referred to herein as R-N BAV; which in humans is associated with a greater degree of complications than

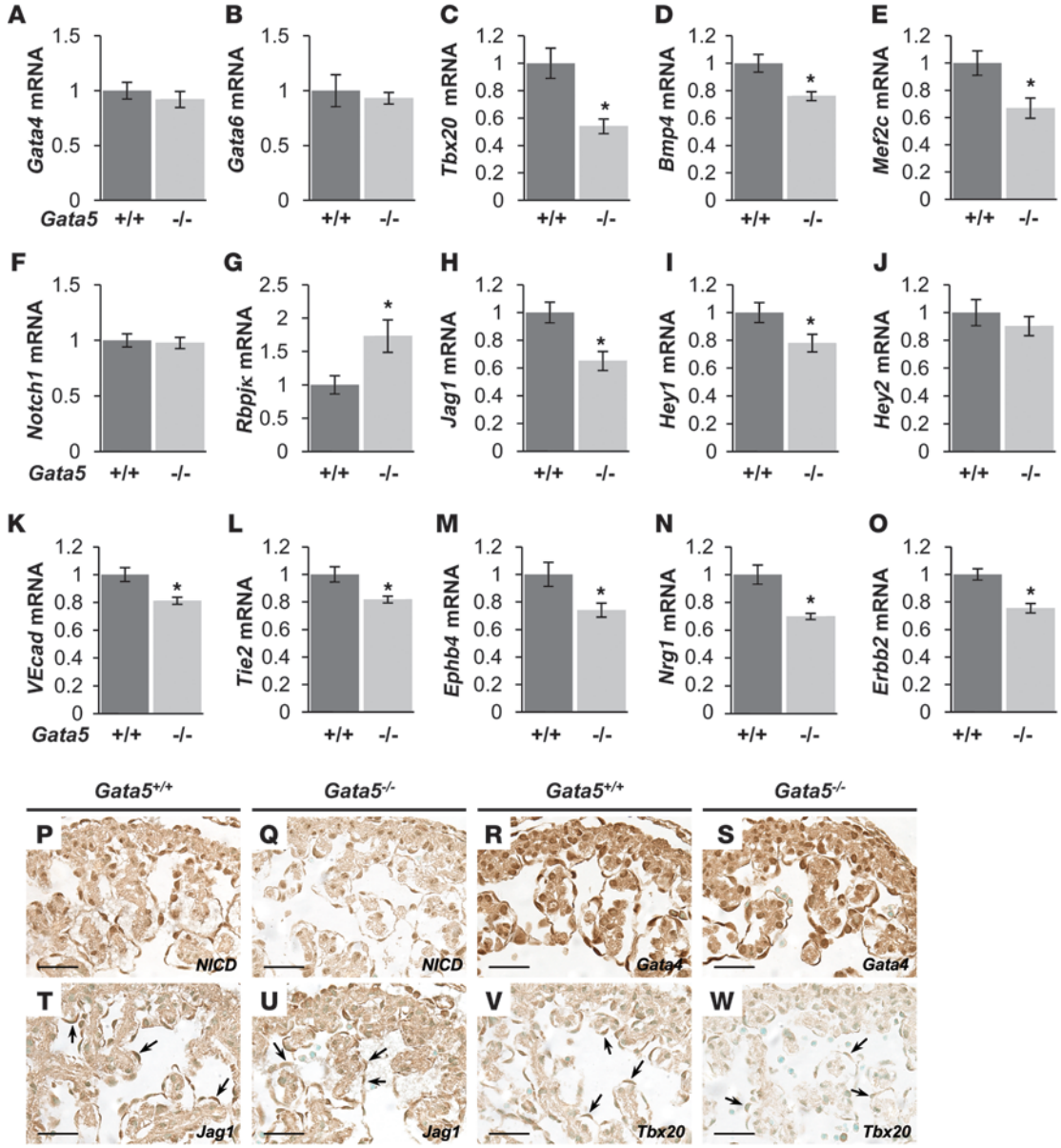

Figure 5

Modulation of gene expression in *Gata5*$^{-/-}$ embryos. (**A**–**E**) Q-PCR showing normal levels of *Gata4* and *Gata6* (**A** and **B**), and altered expression of *Tbx20*, *Bmp4*, and *Mef2c* (**C**–**E**) in the hearts of *Gata5*$^{-/-}$ embryos at E12.5 (n = 6–8 per group). (**F**–**J**) Q-PCR of members of the Notch pathway (n = 6–8 per group). Expression of *Notch1* and *Hey2* remained stable (**F** and **J**), *Rbpjκ* transcripts were significantly upregulated (**G**), and *Jag1* and *Hey1* transcripts were downregulated (**H** and **I**) in *Gata5*$^{-/-}$ embryos at E12.5. (**K**–**O**) Q-PCR showing altered expression of several endothelial markers in *Gata5*$^{-/-}$ embryos at E12.5 (n = 6–8 per group). (**P**–**W**) Transverse sections of E10.5 control and *Gata5*$^{-/-}$ embryos stained for NICD (**P** and **Q**), Gata4 (**R** and **S**), Jag1 (**T** and **U**), and Tbx20 (**V** and **W**). Note the decreased NICD, Jag1, and Tbx20 expression in *Gata5*$^{-/-}$ embryos (**Q**, **U**, and **W**). Scale bars: 40 μm. *P < 0.05 vs. *Gata5*$^{+/+}$.

in other BAV subforms; ref. 38). Next, we verified whether formation of the cardiac jelly, which is critical for EC development, is altered in *Gata5*$^{-/-}$ mice. The cardiac jelly results from EMT, the transformation of a subset of endothelial cells in the endocardium into mesenchymal cells that migrate and invade the extracellular matrix (ECM). Sections of *Gata5*$^{+/+}$ and *Gata5*$^{-/-}$ embryos at E11.5 were stained with alcian blue, which stains acid glycosaminoglycans that mark the EMT (Figure 4, M and N). Alcian blue staining was detected in both control and *Gata5*$^{-/-}$ mice, and there were no major differences between the 2 genotypes, which suggests that Gata5 is not required for cardiac jelly formation. This hypothesis was further supported by the finding that transcripts for *Has-2*, the major component of the cardiac jelly, remained unaltered in *Gata5*$^{-/-}$ hearts at E12.5 (data not shown). Together, these results suggest that Gata5 may regulate genes involved in EC migration and/or differentiation.

Gata5 regulates the Notch pathway. Gene expression patterns in embryonic and postnatal hearts of *Gata5*$^{-/-}$ and control mice were analyzed using Q-PCR. Expression of the 2 other cardiac GATA

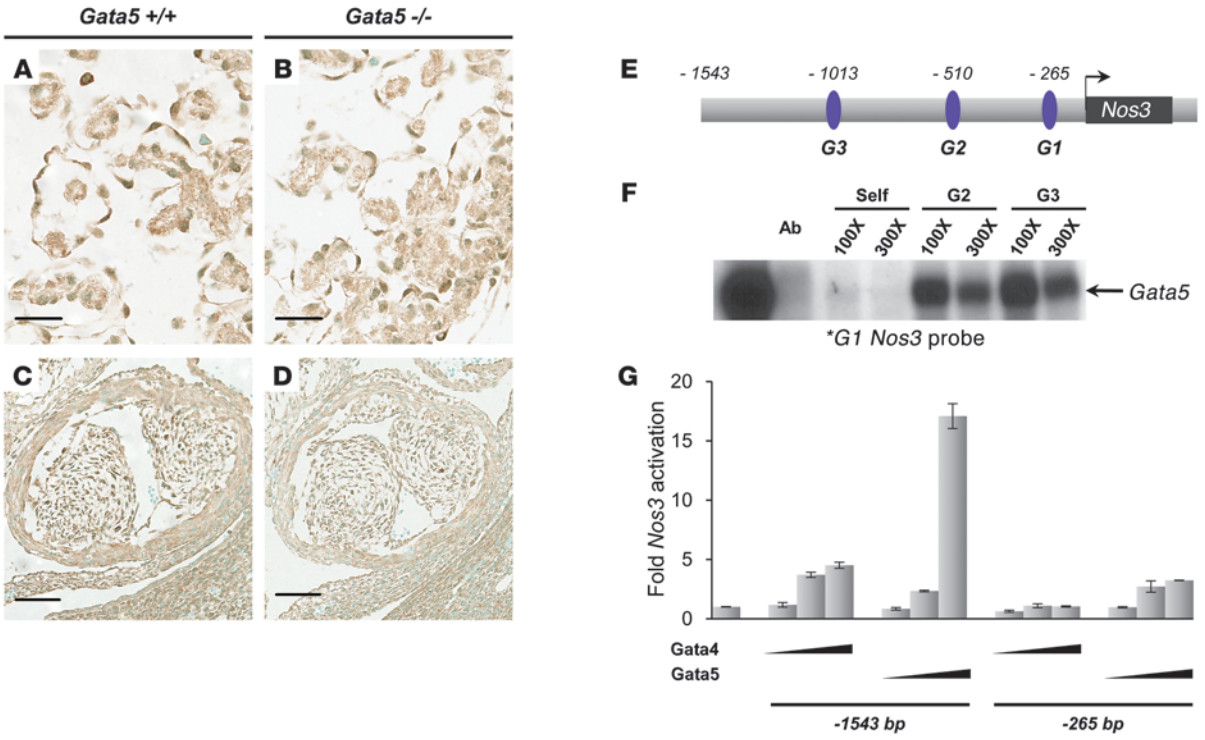

Figure 6
Gata5 regulates *Nos3* expression. (**A** and **B**) Transverse section of E10.5 embryos showing reduced Nos3 expression in ECs of *Gata5*$^{-/-}$ LV. (**C** and **D**) Transverse OFT section of E11.5 embryos showing reduced *Gata5*$^{-/-}$ expression of Nos3. (**E**) Schematic representation of the murine *Nos3* promoter; conserved GATA binding sites are shown. (**F**) DNA binding of Gata5-expressing NIH 3T3 cells on the proximal GATA-binding element of the *Nos3* promoter. Note that binding was displaced by a Gata5-specific Ab or by addition of excess cold probe (self, G2, G3). (**G**) Fold activation of the –1.6 kbp and –265 bp *Nos3* promoter by increasing amounts of Gata4 and Gata5 in NIH 3T3 cells. Data are the average of a duplicate experiment repeated 3 times. Scale bars: 30 μm (**A** and **B**); 75 μm (**C** and **D**).

factors, *Gata4* and *Gata6*, were unchanged in *Gata5*$^{-/-}$ embryonic or adult hearts (Figure 5, A and B, and data not shown). This was confirmed by immunohistochemistry, in which intact levels of *Gata4* were observed in control and *Gata5*$^{-/-}$ embryos (Figure 5, R and S). However, a significant reduction in the mRNA levels of other transcription factors, including *Tbx20* (47%), *Mef2c* (34%), and *Bmp4* (25%), was observed in *Gata5*$^{-/-}$ hearts (Figure 5, C–E). Reduction of *Tbx20* was confirmed in ECs by immunohistochemistry (Figure 5, V and W).

As mentioned earlier, Notch signaling is critical for proper cardiovascular development, and mutations in *NOTCH1*, *NOTCH2*, and the Notch ligand *JAG1* have been associated with OFT defects in humans (8, 18, 39). Moreover, *JAG1* mutations have also been associated with tetralogy of Fallot and pulmonary stenosis (19, 40, 41). We analyzed expression of various Notch components; at E12.5, the mRNA levels of *Notch1*, *Notch2*, *Notch4*, and *Dll4* were similar in *Gata5*$^{-/-}$ and control embryos (Figure 5F and data not shown). However, a 35% decrease in *Jag1* transcripts was observed in *Gata5*$^{-/-}$ embryos (Figure 5H). Moreover, a 2-fold increase in the mRNA of the Notch transcriptional effector *Rbpjκ* was observed (Figure 5G). Given that in the absence of Notch activation, Rbpjκ acts as a transcriptional repressor, the finding that Jag1 expression was decreased while that of Rbpjκ was increased is suggestive dysregulation of the Notch pathway in *Gata5*$^{-/-}$ hearts. Consistent with this, we observed decreased immunostaining for NICD and Jag1 as early as E10.5 (Figure 5, P, Q, T, and U), which confirmed that the Notch pathway was downregulated in *Gata5*$^{-/-}$ mice. Accordingly, a significant decrease in the Notch targets *Nrg1* (30%) and *Hey1* (20%) was found (Figure 5, I and N). Other endothelial and EC markers like *VEcad* (20%), *Tie2* (20%), and *Ephb4* (25%) were also downregulated (Figure 5, K–M).

Endothelial Nos3 plays an important role in AV formation, as shown by the presence in *Nos3*$^{-/-}$ mice of partially penetrant R-N BAVs, the subform of defects seen in *Gata5*$^{-/-}$ mice (12, 38). Nos3 expression was downregulated as early as E10.5 in the LV and the OFT of *Gata5*$^{-/-}$ embryos compared with *Gata5*$^{+/+}$ controls (Figure 6, A–D). Bioinformatic analysis of the murine *Nos3* promoter revealed 3 evolutionarily conserved GATA binding sites (Figure 6E). Gata5 was able to bind to these 3 GATA elements with high affinity (Figure 6F). Additionally, in cotransfection experiments, *Gata5* enhanced *Nos3* promoter activity to a greater extent than did *Gata4* (18- vs. 5-fold activation; Figure 6G). The results identified *Nos3* as a Gata5 target and suggest that reduction in Nos3 may be a contributing mechanism to BAVs.

Endocardial Gata5 is required for AV formation. Formation of the OFT cushion is accompanied by migration of mesenchymal cells from the neural crest, the pharyngeal mesenchyme, and endocardial derived mesenchyme. To determine which cell type is responsible for the formation of BAVs in *Gata5*$^{-/-}$ mice, we mutated the *Gata5* gene specifically in endothelial cells by crossing with *Tie2-cre* transgenic mice to obtain *Tie2-cre*$^{+}$*Gata5*$^{fl/fl}$ mice.

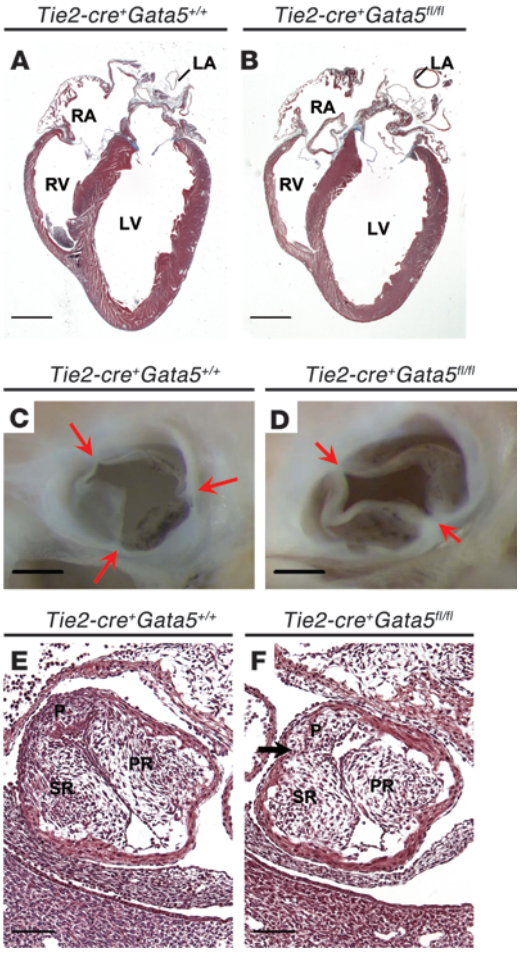

Figure 7
Gata5 is required in ECs for AV formation. (**A** and **B**) Trichrome staining of *Tie2-cre*$^{+}$*Gata5*$^{+/+}$ and *Tie2-cre*$^{+}$*Gata5*$^{fl/fl}$ frontal sections. There were no major differences between groups in heart size or wall thickness. (**C** and **D**) Anatomical analysis revealed the presence of BAV in *Tie2-cre*$^{+}$*Gata5*$^{fl/fl}$ mice. Arrows denote points of attachment of the valve cups to the aortic wall. (**E** and **F**) Trichrome staining of transverse sections of OFT at E11.5. Arrow denotes abnormal fusion of the posterior intercalated cushion with the septal ridge, creating a R-N BAV. Scale bars: 1,500 μm (**A** and **B**); 400 μm (**C** and **D**); 75 μm (**E** and **F**).

This approach was selected because Gata5 is enriched in ECs, but absent from vascular endothelial and neural crest cells (35, 36). In mice carrying the *Tie2-cre* transgene, recombination occurs as early as E9.5 in ECs of both the OFT and AVC that will eventually give rise to the semilunar (pulmonary and aortic) and atrioventricular (mitral and tricuspid) valves (42). *Tie2-cre*$^{+}$*Gata5*$^{fl/fl}$ mice were obtained at the expected Mendelian ratios and were viable. As in *Gata5*$^{-/-}$ mice, we found BAVs in 21% (3 of 14) of *Tie2-cre*$^{+}$*Gata5*$^{fl/fl}$ mice compared with 3% (1 of 31) of control *Tie2-cre*$^{+}$*Gata5*$^{+/+}$ littermates (Figure 7, C and D, and Table 2). Close examination of the morphology of the OFT cushions of *Tie2-cre*$^{+}$*Gata5*$^{fl/fl}$ embryos at E11.5 yielded results identical to those of *Gata5*$^{-/-}$ embryos, namely, abnormal fusion between the posterior intercalated cushion and the septal ridge creating an R-N BAV (Figure 7, E and F).

Q-PCR analysis for exons 4–6 in E12.5 *Tie2-cre*$^{+}$*Gata5*$^{fl/fl}$ embryos confirmed strong downregulation of *Gata5* transcripts with low residual expression (Figure 8A). At the cell level, immunostaining with the anti-Gata5 antibody indicated that *Gata5* expression was significantly reduced in most ECs as early as E10.5 (Figure 8, G–J). No significant change in *Gata4* and *Gata6* transcript levels was noted in *Tie2-cre*$^{+}$*Gata5*$^{fl/fl}$ embryos (Figure 8, B and C). However, a strong downregulation of *Tbx20* (50%) and *Jag1* (50%) transcripts and a significant decrease in *Erbb2* (30%) mRNA was detected in these hearts (Figure 8, D–F). Immunostaining confirmed that Jag1 expression was downregulated in *Tie2-cre*$^{+}$*Gata5*$^{fl/fl}$ embryos at E10.5 (Figure 8, M and N). In addition, reduced expression of NICD was noted in these embryos (Figure 8, K and L), indicative of defective Notch pathway.

Together, these results indicate that Gata5 is an important regulator of genes involved in EC differentiation and that expression of Gata5 in ECs is required for proper development of the endocardial cushions. Moreover, the data suggest that absence of Gata5 results in defective valve morphogenesis and BAV formation.

Discussion

In this study, we used mouse genetics to determine the function of Gata5 in mammalian embryogenesis. The results revealed an essential role for Gata5 in heart morphogenesis and a critical cell-autonomous role in endocardial cushion formation and AV development. In particular, we showed that deletion of *Gata5* resulted in BAV formation. In humans, most BAVs result from fusion of either the right-coronary and left-coronary leaflets (R-L) or the right-coronary and noncoronary leaflet (R-N). R-N BAV is associated with a greater degree of valve dysfunction, and it has also become clear over the years that BAV morphology is of prognostic relevance in the management of patients with BAVs (43–45). Work in animal models suggests that the 2 subtypes may be distinct etiological entities; R-N BAVs would result from defective development of the cardiac OFT endocardial cushions, whereas R-L BAVs result from an extra fusion of the septal and parietal ridges (38). The BAVs in *Gata5*$^{-/-}$ mice were, in all cases, the result of a fusion between the posterior intercalated cushion and the septal ridge, giving rise to the R-N subtype. The differential formation of R-N BAVs supports the hypothesis that the different BAV subtypes have distinct genetic etiologies. As a corollary, differential outcomes in humans with R-N BAVs and R-L BAVs may be due to distinct underlying genetic pathways.

Cardiac valves are derived from the endocardial cushions, which are rich in ECM components. Defective development of the heart valves occurs in 20%–30% of all CHDs (46, 47). There is increasing evidence that loss of ECM organization is associated with changes in mechanical properties, leading to dysfunction in adult valve disease.

Table 2
BAV incidence in *Tie2-cre*$^{+}$*Gata5*$^{+/+}$ and *Tie2-cre*$^{+}$*Gata5*$^{fl/fl}$ mice

Genotype	Total mice	Mice with BAV	Incidence
Tie2-cre^{+}*Gata5*$^{+/+}$	31	1	3%
Tie2-cre^{+}*Gata5*$^{fl/fl}$	14	3	21%

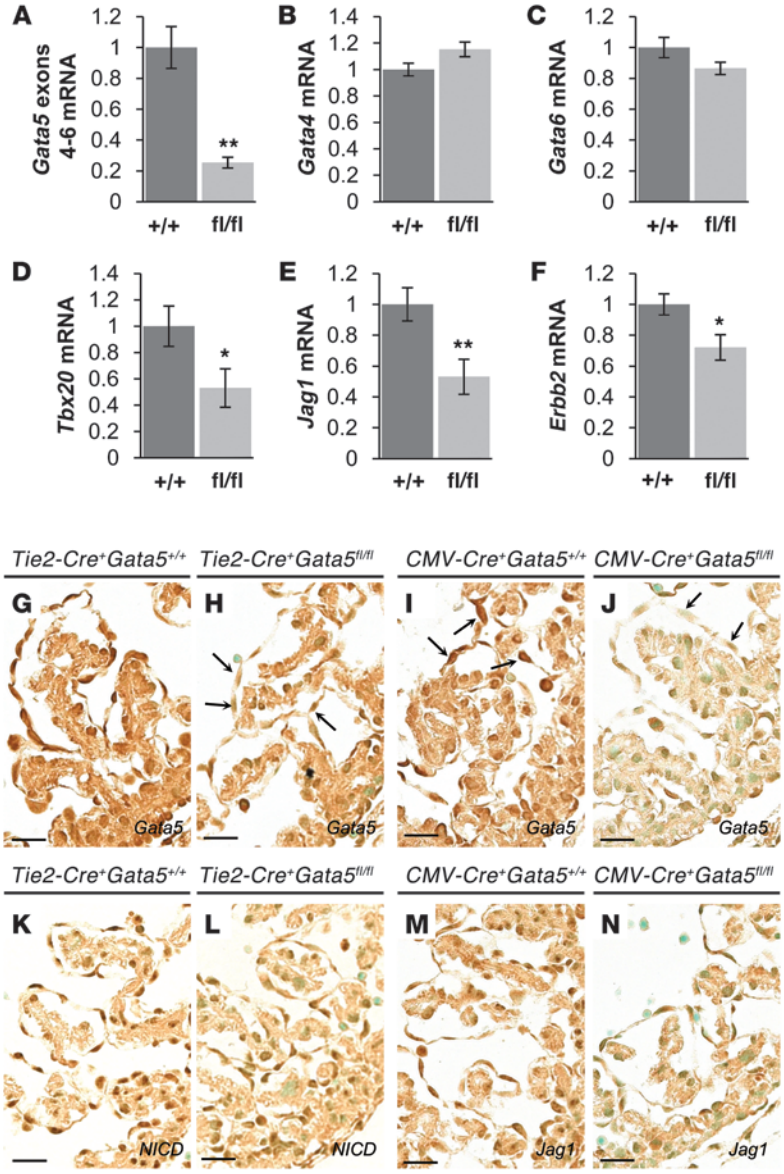

Figure 8
Modulation of gene expression in *Tie2-cre*$^{+}$*Gata5*$^{fl/fl}$ embryos. (**A**–**C**) Q-PCR showed strong reduction of *Gata5* transcripts (**A**) in *Tie2-cre*$^{+}$*Gata5*$^{+/+}$ and *Tie2-cre*$^{+}$*Gata5*$^{fl/fl}$ embryos at E12.5 (n = 6–7 per group). Expression of *Gata4* (**B**) and *Gata6* (**C**) mRNA remained normal in *Tie2-cre*$^{+}$*Gata5*$^{fl/fl}$ embryos. (**D**–**F**) Q-PCR showed strong reduction of *Tbx20* (**D**) and *Jag1* (**E**) transcripts in *Tie2-cre*$^{+}$*Gata5*$^{fl/fl}$ embryos at E12.5. *Erbb2* transcripts (**F**) were significantly downregulated (n = 6–7 per group). (**G**–**J**) Gata5 immunostaining of E11.5 transverse sections. Note the reduction of Gata5 in *Tie2-cre*$^{+}$*Gata5*$^{fl/fl}$ embryos and its absence in *CMV-cre*$^{+}$*Gata5*$^{fl/fl}$ embryos. (**K**–**N**) Immunostaining of E11.5 transverse sections of control and *Tie2-cre*$^{+}$*Gata5*$^{fl/fl}$ embryos for NICD and Jag1. Expression of both antibodies was reduced in the *Tie2-cre*$^{+}$*Gata5*$^{fl/fl}$ embryos. Scale bars: 20 μm. $^{*}P < 0.05$, $^{**}P < 0.01$.

A number of studies have shown that periostin is required for normal cardiac valve development and maturation (48, 49). Valve leaflets of *periostin*$^{-/-}$ mice are hypertrophied and shortened by 3 months of age, and the tendinous cords of the AVs are either truncated or missing. The phenotype of *periostin*$^{-/-}$ mice is similar to the degenerative changes seen in prolapsed human mitral valves or BAVs. Periostin levels are also pathologically overexpressed in infiltrated inflammatory cells and myofibroblasts in areas of angiogenesis in human atherosclerosis and rheumatic valve disease (50). Versican, another EMC component, plays important roles during cardiac development and in adult cardiovascular diseases (51, 52). Versican cleavage occurs throughout cardiac development by members of the ADAMTS family, such as *Adamts9*, which is expressed in mesenchymal cells of the valves. *Adamst9* haploinsufficiency leads to abnormal thickening of the semilunar valve leaflets as well as to increased proteoglycan content in the AV (53). Proper elastic fiber assembly and function are critical for AV and aortic wall integrity. Mutations in elastins, fibulin family members, and other components of elastic fiber assembly result in progressive adult disease — including supravalvar stenosis — in animal models and in humans (54, 55). No significant changes in mRNA levels for *periostin*, *elastin*, and several other ECM-relevant genes were found in *Gata5*$^{-/-}$ embryonic hearts. Whether changes develop in aging *Gata5*$^{-/-}$ mice deserves to be assessed.

Valve development requires complex interactions between transcription factors that regulate proliferation, differentiation, and leaflet remodeling. Gata5 appears to regulate at least 2 pathways involved in differentiation of ECs, namely, Tbx20 and Notch. Tbx20, a member of the T-box gene family, is expressed in myocardial cells as well as ECs during avian and mammalian development. Deletion of *Tbx20* in mice results in embryonic lethality, reduced myocardial differentiation, and defective chamber maturation (56). Knockdown of *Tbx20* with siRNAs provided the first evidence for Tbx20 involvement in valve development (57). More recently, 2 studies showed that Tbx20 was required for proliferation and migration of mesenchymal cells within the cushions (28, 58).

Importantly, mutations in the *TBX20* gene have been linked with valve and septal defects in humans (59, 60). Our results showed a 45% reduction of *Tbx20* transcripts in *Gata5*$^{-/-}$ and *Tie2-cre*$^{+}$*Gata5*$^{fl/fl}$ embryos along with a reduced number of mesenchymal cells in both the AVC and OFT cushions at E12.5. Thus, Tbx20 may be a downstream target of Gata5 in ECs. Another critical regulator of valvulogenesis is the Notch pathway. Mutations in the *NOTCH1* gene have been associated with BAV in humans, and mutations in *JAG1* and *NOTCH2* have been associated with Alagille syndrome, which is characterized by multiple OFT defects (8, 18, 39). Gata5 and Jag1 are both expressed in endothelial cells and endocardial cushion cells of the OFT and AVC at E12.5; our study revealed substantial downregulation of *Jag1* transcripts in *Gata5*$^{-/-}$ and *Tie2-cre*$^{+}$*Gata5*$^{fl/fl}$ embryos, with concomitant upregulation of the transcriptional repressor Rbpjκ (36, 61). Decreased ligand levels, together with upregulation of the transcriptional repressor, would be expected to result in significant attenuation of the functional Notch pathway in ECs. In this respect, it is noteworthy that loss of Notch1 or Rbpjκ from ECs and endothelial cells was previously shown to result in hypotrabeculated, hypoplastic hearts (22). Our results are in line with this study and support a regulatory function for endocardial Notch signaling in myocardial morphogenesis.

Finally, the data presented herein confirm a role for Gata5 in EC differentiation in vivo, which is consistent with our previous in vitro work and with the phenotype of the zebrafish *faust* mutant, which encodes Gata5 (36, 37). However, the phenotype of our *Gata5*$^{-/-}$ mice differ from that of a previously described *Gata5*$^{-/-}$ line that displayed no overt cardiac phenotype (62). The *Gata5* locus produces 2 protein isoforms through alternative translation initiation; in addition to the translation start site in exon 1, use of a second ATG upstream of exon 2 generates a truncated Gata5 protein composed of aa 225–404, which retains 1 zinc finger as well as DNA binding and transcriptional activation properties (63, 64). In contrast to the targeting strategy used by Molkentin et al. (62), which only deletes 1 isoform, our strategy was designed to delete exons 3–6, which contain the DNA binding, nuclear localization, and C-terminal transactivation domains, therefore ensuring that both isoforms are eliminated. While the present study was in progress, another group reported the production of mice carrying a *Gata5*^{tm2Eem} mutated allele that deletes both zinc finger coding exons (65). The *Gata5*^{tm2Eem} mice did not display an apparent cardiac phenotype, but showed 2-fold overexpression of both *Gata4* and *Gata6* mRNA. Crossing these into a *Gata4*$^{+/-}$ background produced hypoplastic ventricles and severe endocardial cushion defects, a phenotype resembling that of our *Gata5*$^{-/-}$ mice. This raises the possibility that upregulation of the other cardiac GATA factor may have compensated for lack of Gata5. In our *Gata5*$^{-/-}$ hearts, we did not detect any changes in Gata4 or Gata6 levels in embryonic or postnatal hearts. Moreover, female *Gata5*$^{-/-}$ mice did not show a reduction in the distance between the vagina and anus, as observed in the other *Gata5* mutated alleles. At present, the reasons for the differential phenotype remain unclear, but the contribution of genetic background to manifestation of CHD is well documented (31). Be that as it may, the results of the present study suggest that Gata5 activity within the proximal and distal OFT is important for development of the AV and, for the first time to our knowledge, document the role of ECs in the pathogenesis of BAVs.

Gata5 is broadly but transiently expressed in ECs and endocardial cushion cells of the AVC and OFT (35, 36). The *Gata5*$^{-/-}$ mice did not display detectable defects in other endocardial derived structures, such as the atrial septum or other valves. Our results suggest that the number of ECs and EMT was not altered in the absence of Gata5; rather, it appears that differentiation and possibly migration or cell-cell interactions are disrupted. It is possible that Gata4 may be able to partially compensate for Gata5 in earlier stages of EC expansion and differentiation; alternatively, the window of Gata5 expression during development may affect only a subgroup of genes and processes involved in OFT development, such as interactions with the secondary heart field or with neural crest–derived cells. Either way, the finding that loss of Gata5 from ECs differentially affected AV leaflets will help in furthering our limited understanding of how common endocardial cushions contribute to specific valve leaflets.

In conclusion, the data presented here are consistent with a crucial role for Gata5 in AV formation and suggest that *GATA5* may be a disease-causing gene. Future studies aimed at elucidating the upstream regulators and downstream targets of Gata5 in ECs will contribute to mechanistic understanding of endocardial cushion development as well as gene pathways involved in BAV and other valve diseases.

Methods

Animals. Mouse handling and experimentation were performed in accordance with institutional guidelines. All protocols were approved by the IACUC of the University of Ottawa and the Institut de recherches cliniques de Montréal.

Histology. Adult tissues or staged mouse embryos at E10.5 and E11.5 were fixed in 4% paraformaldehyde, paraffin embedded, sectioned at 4-μm intervals, and processed as previously described (35). Anti-Gata4, anti-Gata5, and anti-Tbx20 antibodies were previously described (35, 57, 66). Polyclonal anti-eNOS, Notch1 NICD, and Jag1 were purchased from Abcam (catalog nos. ab66127, ab8925, and ab7771, respectively). The biotinylated anti-rabbit IgG antibody was purchased from Vector Laboratories (BA1000).

Cell count. Image J software was used to count the number of myocytes, ECs, and cushions cells in 3 different sections of 3–4 different heart samples per genotype.

Gel shift assay. Nuclear extracts of NIH 3T3 cells overexpressing Gata5 were obtained as previously described (35). The probe used for GATA binding (5′- GTTCCCACTTATCAGCTCTAGCCC-3′) corresponded to the –265 GATA element (underline).

Generation of Gata5 mutant mice. The detailed strategy for generating mice lacking *Gata5* is described in Supplemental Methods. Mice were kept on a mixed 129SV/C57BL/6 background.

BAV and tricuspid AV analysis. Hearts were perfused with 4% paraformaldehyde in PBS and then fixed overnight at 4°C. Atria were removed under the microscope, and the aortic arch and pulmonary artery were cut at an angle to reveal the AV.

Echocardiography. Transthoracic echocardiography was performed using a visual sonics Vevo 770 ultrasound system with a RMV 707 30-MHz transducer as previously described (66). Doppler and M-mode imaging was obtained from 70-day-old mice. Statistical analysis was done using Student's 2-tailed *t* test. Groups of 11–14 mice from different litters were used for the M-mode measurements and Doppler readings at 70 days.

Q-PCR. Total RNA was isolated from hearts of E12.5 embryos or from LV and IVS at postnatal day 30 with TRIzol reagent (Invitrogen); cDNAs were generated using the Omniscript RT kit (Qiagen), and Q-PCR was performed as previously described (67). See Supplemental Table 1 for primer sequences.

Statistics. Values are presented as mean ± SEM. *P* values were generated using Student's 2-tailed *t* test, and *P* values less than 0.05 were considered statistically significant.

Acknowledgments

We are grateful to Quinzhang Zhu for ES cell selection and blastocyst injection, Manon Laprise for echocardiography measurements, Annie Vallée and Geneviève Brindle for help with histology, Chantal Lefebvre for genotyping, and Lise Laroche and Hélène Touchette for expert secretarial work. We thank Marie Kmita, Céline Fiset, and Salim Hayek as well as the Nemer lab for discussions and helpful suggestions. G. Andelfinger is a clinician scientist of the Canadian Institutes for Health Research (CIHR). M. Nemer was recipient of a Canada Research Chair in cardiac growth and differentiation. This work was supported by grants from CIHR (MOP36382 and GMD 79045) and by the Heart and Stroke Foundation of Ontario.

Received for publication July 29, 2010, and accepted in revised form April 4, 2011.

Address correspondence to: Mona Nemer, Department of Biochemistry, Microbiology, and Immunology, University of Ottawa, 550 Cumberland (246), Ottawa, Ontario K1N 6N5, Canada. Phone: 613.562.5270; Fax: 613.562.5271; E-mail: mona.nemer@uottawa.ca.

1. De MP, Longo UG, Galanti G, Maffulli N. Bicuspid aortic valve: a literature review and its impact on sport activity. *Br Med Bull*. 2008;85:63–85.
2. Ward C. Clinical significance of the bicuspid aortic valve. *Heart*. 2000;83(1):81–85.
3. Hinton RB, Martin LJ, Rame-Gowda S, Tabangin ME, Cripe LH, Benson DW. Hypoplastic left heart syndrome links to chromosomes 10q and 6q and is genetically related to bicuspid aortic valve. *J Am Coll Cardiol*. 2009;53(12):1065–1071.
4. Tadros TM, Klein MD, Shapira OM. Ascending aortic dilatation associated with bicuspid aortic valve: pathophysiology, molecular biology, and clinical implications. *Circulation*. 2009;119(6):880–890.
5. Hor KN, Border WL, Cripe LH, Benson DW, Hinton RB. The presence of bicuspid aortic valve does not predict ventricular septal defect type. *Am J Med Genet A*. 2008;146A(24):3202–3205.
6. Clementi M, Notari L, Borghi A, Tenconi R. Familial congenital bicuspid aortic valve: a disorder of uncertain inheritance. *Am J Med Genet*. 1996;62(4):336–338.
7. Cripe L, Andelfinger G, Martin LJ, Shooner K, Benson DW. Bicuspid aortic valve is heritable. *J Am Coll Cardiol*. 2004;44(1):138–143.
8. Garg V, et al. Mutations in NOTCH1 cause aortic valve disease. *Nature*. 2005;437(7056):270–274.
9. Mohamed SA, et al. Novel missense mutations (p.T596M and p.P1797H) in NOTCH1 in patients with bicuspid aortic valve. *Biochem Biophys Res Commun*. 2006;345(4):1460–1465.
10. Martin LJ, et al. Evidence in favor of linkage to human chromosomal regions 18q, 5q and 13q for bicuspid aortic valve and associated cardiovascular malformations. *Hum Genet*. 2007;121(2):275–284.
11. Biben C, et al. Cardiac septal and valvular dysmorphogenesis in mice heterozygous for mutations in the homeobox gene Nkx2-5. *Circ Res*. 2000; 87(10):888–895.
12. Lee TC, Zhao YD, Courtman DW, Stewart DJ. Abnormal aortic valve development in mice lacking endothelial nitric oxide synthase. *Circulation*. 2000;101(20):2345–2348.
13. Combs MD, Yutzey KE. Heart valve development: regulatory networks in development and disease. *Circ Res*. 2009;105(5):408–421.
14. Dor Y, Klewer SE, McDonald JA, Keshet E, Camenisch TD. VEGF modulates early heart valve formation. *Anat Rec A Discov Mol Cell Evol Biol*. 2003;271(1):202–208.
15. Dor Y, et al. A novel role for VEGF in endocardial cushion formation and its potential contribution to congenital heart defects. *Development*. 2001; 128(9):1531–1538.
16. Li L, et al. Alagille syndrome is caused by mutations in human Jagged1, which encodes a ligand for Notch1. *Nat Genet*. 1997;16(3):243–251.
17. Oda T, Elkahloun AG, Meltzer PS, Chandrasekharappa SC. Identification and cloning of the human homolog (JAG1) of the rat Jagged1 gene from the Alagille syndrome critical region at 20p12. *Genomics*. 1997;43(3):376–379.
18. McDaniell R, et al. NOTCH2 mutations cause Alagille syndrome, a heterogeneous disorder of the notch signaling pathway. *Am J Hum Genet*. 2006;79(1):169–173.
19. Eldadah ZA, et al. Familial Tetralogy of Fallot caused by mutation in the jagged1 gene. *Hum Mol Genet*. 2001;10(2):163–169.
20. Krantz ID, et al. Jagged1 mutations in patients ascertained with isolated congenital heart defects. *Am J Med Genet*. 1999;84(1):56–60.
21. High FA, Epstein JA. The multifaceted role of Notch in cardiac development and disease. *Nat Rev Genet*. 2008;9(1):49–61.
22. Grego-Bessa J, et al. Notch signaling is essential for ventricular chamber development. *Dev Cell*. 2007;12(3):415–429.
23. Schilham MW, et al. Defects in cardiac outflow tract formation and pro-B-lymphocyte expansion in mice lacking Sox-4. *Nature*. 1996;380(6576):711–714.
24. Seo S, Fujita H, Nakano A, Kang M, Duarte A, Kume T. The forkhead transcription factors, Foxc1 and Foxc2, are required for arterial specification and lymphatic sprouting during vascular development. *Dev Biol*. 2006;294(2):458–470.
25. Wang B, et al. Foxp1 regulates cardiac outflow tract, endocardial cushion morphogenesis and myocyte proliferation and maturation. *Development*. 2004;131(18):4477–4487.
26. Harrelson Z, et al. Tbx2 is essential for patterning the atrioventricular canal and for morphogenesis of the outflow tract during heart development. *Development*. 2004;131(20):5041–5052.
27. Ribeiro I, et al. Tbx2 and Tbx3 regulate the dynamics of cell proliferation during heart remodeling. *PLoS ONE*. 2007;2(4):e398.
28. Shelton EL, Yutzey KE. Tbx20 regulation of endocardial cushion cell proliferation and extracellular matrix gene expression. *Dev Biol*. 2007;302(2):376–388.
29. Rivera-Feliciano J, et al. Development of heart valves requires Gata4 expression in endothelial-derived cells. *Development*. 2006;133(18):3607–3618.
30. Nemer G, et al. A novel mutation in the *GATA4* gene in patients with tetralogy of Fallot. *Hum Mutat*. 2006;27(3):293–294.
31. Rajagopal SK, et al. Spectrum of heart disease associated with murine and human GATA4 mutation. *J Mol Cell Cardiol*. 2007;43(6):677–685.
32. Tomita-Mitchell A, Maslen CL, Morris CD, Garg V, Goldmuntz E. GATA4 sequence variants in patients with congenital heart disease. *J Med Genet*. 2007;44(12):779–783.
33. Kodo K, et al. GATA6 mutations cause human cardiac outflow tract defects by disrupting semaphorin-plexin signaling. *Proc Natl Acad Sci U S A*. 2009;106(33):13933–13938.
34. Morrisey EE, Ip HS, Tang ZH, Lu MM, Parmacek MS. GATA-5 - a transcriptional activator expressed in a novel temporally and spatially-restricted pattern during embryonic development. *Dev Biol*. 1997;183(1):21–36.
35. Nemer G, Nemer M. Transcriptional activation of BMP-4 and regulation of mammalian organogenesis by GATA-4 and -6. *Dev Biol*. 2003;254(1):131–148.
36. Nemer G, Nemer M. Cooperative interaction between GATA-5 and NF-ATc regulates endothelial-endocardial differentiation of cardiogenic cells. *Development*. 2002;129(17):4045–4055.
37. Reiter JF, et al. Gata5 is required for the development of the heart and endoderm in zebrafish. *Genes Dev*. 1999;13(22):2983–2995.
38. Fernandez B, et al. Bicuspid aortic valves with different spatial orientations of the leaflets are distinct etiological entities. *J Am Coll Cardiol*. 2009; 54(24):2312–2318.
39. Warthen DM, et al. Jagged1 (JAG1) mutations in Alagille syndrome: increasing the mutation detection rate. *Hum Mutat*. 2006;27(5):436–443.
40. Bauer RC, et al. Jagged1 (JAG1) mutations in patients with tetralogy of Fallot or pulmonic stenosis. *Hum Mutat*. 2010;31(5):594–601.
41. Sousa AB, Medeira A, Kamath BM, Spinner NB, Cordeiro I. Familial stenosis of the pulmonary artery branches with a JAG1 mutation. *Rev Port Cardiol*. 2006;25(4):447–452.
42. Kisanuki YY, Hammer RE, Miyazaki J, Williams SC, Richardson JA, Yanagisawa M. Tie2-Cre transgenic mice: a new model for endothelial cell-lineage analysis in vivo. *Dev Biol*. 2001;230(2):230–242.
43. Sans-Coma V, et al. Fusion of valve cushions as a key factor in the formation of congenital bicuspid aortic valves in Syrian hamsters. *Anat Rec*. 1996; 244(4):490–498.
44. Russo CF, Cannata A, Lanfranconi M, Vitali E, Garatti A, Bonacina E. Is aortic wall degeneration related to bicuspid aortic valve anatomy in patients with valvular disease? *J Thorac Cardiovasc Surg*. 2008;136(4):937–942.
45. Fernandes SM, Khairy P, Sanders SP, Colan SD. Bicuspid aortic valve morphology and interventions in the young. *J Am Coll Cardiol*. 2007;49(22):2211–2214.
46. Pierpont ME, et al. Genetic basis for congenital heart defects: current knowledge: a scientific statement from the American Heart Association Congenital Cardiac Defects Committee, Council on Cardiovascular Disease in the Young: endorsed by the American Academy of Pediatrics. *Circulation*. 2007; 115(23):3015–3038.
47. Hoffman JI, Kaplan S. The incidence of congenital heart disease. *J Am Coll Cardiol*. 2002; 39(12):1890–1900.
48. Norris RA, et al. Periostin regulates atrioventricular valve maturation. *Dev Biol*. 2008;316(2):200–213.
49. Snider P, et al. Periostin is required for maturation and extracellular matrix stabilization of noncardiomyocyte lineages of the heart. *Circ Res*. 2008; 102(7):752–760.
50. Hakuno D, et al. Periostin advances atherosclerotic and rheumatic cardiac valve degeneration by inducing angiogenesis and MMP production in humans and rodents. *J Clin Invest*. 2010;120(7):2292–2306.
51. Eronen M, et al. Cardiovascular manifestations in 75 patients with Williams syndrome. *J Med Genet*. 2002;39(8):554–558.
52. Hinton RB, et al. Elastin haploinsufficiency results in progressive aortic valve malformation and latent valve disease in a mouse model. *Circ Res*. 2010;107(4):549–557.

53. Kern CB, et al. Reduced versican cleavage due to Adamts9 haploinsufficiency is associated with cardiac and aortic anomalies. *Matrix Biol*. 2010;29(4):304–316.
54. Urban Z, et al. Connection between elastin haploinsufficiency and increased cell proliferation in patients with supravalvular aortic stenosis and Williams-Beuren syndrome. *Am J Hum Genet*. 2002;71(1):30–44.
55. Huang J, et al. Genetic modification of mesenchymal stem cells overexpressing CCR1 increases cell viability, migration, engraftment, and capillary density in the injured myocardium. *Circ Res*. 2010;106(11):1753–1762.
56. Singh MK, et al. Tbx20 is essential for cardiac chamber differentiation and repression of Tbx2. *Development*. 2005;132(12):2697–2707.
57. Takeuchi JK, et al. Tbx20 dose-dependently regulates transcription factor networks required for mouse heart and motoneuron development. *Development*. 2005;132(10):2463–2474.
58. Shelton EL, Yutzey KE. Twist1 function in endocardial cushion cell proliferation, migration, and differentiation during heart valve development. *Dev Biol*. 2008;317(1):282–295.
59. Kirk EP, et al. Mutations in cardiac T-box factor gene TBX20 are associated with diverse cardiac pathologies, including defects of septation and valvulogenesis and cardiomyopathy. *Am J Hum Genet*. 2007;81(2):280–291.
60. Posch MG, et al. A gain-of-function TBX20 mutation causes congenital atrial septal defects, patent foramen ovale and cardiac valve defects. *J Med Genet*. 2010;47(4):230–235.
61. Loomes KM, et al. The expression of Jagged1 in the developing mammalian heart correlates with cardiovascular disease in Alagille syndrome. *Hum Mol Genet*. 1999;8(13):2443–2449.
62. Molkentin JD, Tymitz KM, Richardson JA, Olson EN. Abnormalities of the genitourinary tract in female mice lacking GATA5. *Mol Cell Biol*. 2000;20(14):5256–5260.
63. Nemer G, Qureshi SA, Malo D, Nemer M. Functional analysis and chromosomal mapping of *GATA5*, a gene encoding a zinc finger DNA-binding protein. *Mamm Genome*. 1999;10(10):993–999.
64. Chen B, et al. Alternative promoter and GATA5 transcripts in mouse. *Am J Physiol Gastrointest Liver Physiol*. 2009;297(6):G1214–G1222.
65. Singh MK, et al. Gata4 and Gata5 cooperatively regulate cardiac myocyte proliferation in mice. *J Biol Chem*. 2010;285(3):1765–1772.
66. Aries A, Paradis P, Lefebvre C, Schwartz RJ, Nemer M. Essential role of GATA-4 in cell survival and drug-induced cardiotoxicity. *Proc Natl Acad Sci U S A*. 2004;101(18):6975–6980.
67. Nadeau M, et al. An endocardial pathway involving Tbx5, Gata4, and Nos3 required for atrial septum formation. *Proc Natl Acad Sci U S A*. 2010;107(45):19356–19361.